Supporting Information

A Multi-responsive Tb-doped MOF Probe for Highly Specific Breath Volatile Biomarkers Recognition of Lung Cancer

Luping Liu[a], Lihua Ru[a], Hanxiao Tang[b], Zhijuan Zhang*[a,c], Weisheng Feng[a]

a. College of Pharmacy, Henan University of Chinese Medicine, Zhengzhou 450046, China

b. College of Chinese Medical Sciences, Henan University of Chinese Medicine, Zhengzhou 450046, China

c. Institute of Mass Spectrometer and Atmospheric Environment, Jinan University, Guangzhou 510632, China

Corresponding author: Zhijuan Zhang, Email: zhangyan0204@126.com (Z. J. Zhang).

1. Materials

N,N'-dimethylformamide (DMF), ethanol, styrene and ethylbenzene of the benzene compounds and the other chemicals all were purchased from J&K Scientific. All reagents and chemicals were analytical reagent and directly used without further purification. Deionized water was prepared from the Milli-Q ultrapure water system throughout all experiments. And the 70 % ethanol used in this experiment was further prepared by anhydrous ethanol by adding deionized water.

2. Methods

All chemicals were purchased and directly used. The inductively coupled plasma optical emission spectrometer (ICP-OES) were measured by Agilent 5110. The powder X-ray diffraction (PXRD) patterns were obtained by Bruker D8 Advance Conventional Angle X-ray diffractometer. Scanning electron microscope (SEM) were measured by TESCAN MIRA LMS. Fourier transform infrared spectroscopy (FTIR) were obtained from Bruker TENSOR Ⅱ instrument. X-ray photoelectron spectra (XPS) were recorded on a Thermo Scientific ESCALAB 250Xi instrument (Thermo Scientific, America) with a monochromatic Al Kα X-ray source (1486.6 eV). Fluorescence lifetime was recorded on an Edinburgh FLS980 instrument by using a microsecond lamp to scan at Ex=269 nm. Fluorescence sensing was recorded on a HITACHI F7100 spectrophotometer.

3. Synthesis of Tb-UiO-66

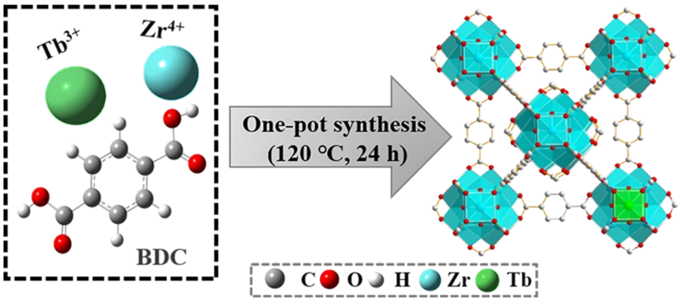

Scheme S1. Synthesis process of Tb-UiO-66.

Table S1. Mole and volume of reagent used to synthesize bimetallic materials Tb-UiO-66.

Sample	Metal source		Ligand	Total solvent	Tb/Zr	
	$ZrCl_4$ (mmol)	$Tb(NO_3)_3•6H_2O$ (mmol)	BDC (mmol)	DMF (mL)	Theoretical ratio	Real ratio (ICP-OES)
Tb-UiO-66 (1:103)	0.061	1.159	1.22	50	1:19	1:103
Tb-UiO-66 (1:65)	0.122	1.098	1.22	50	1:9	1:65
Tb-UiO-66 (1:17)	0.305	0.915	1.22	50	1:3	1:17
Tb-UiO-66 (1:1.5)	0.610	0.610	1.22	50	1:1	1:1.5

4. Chemical stability Tb-UiO-66

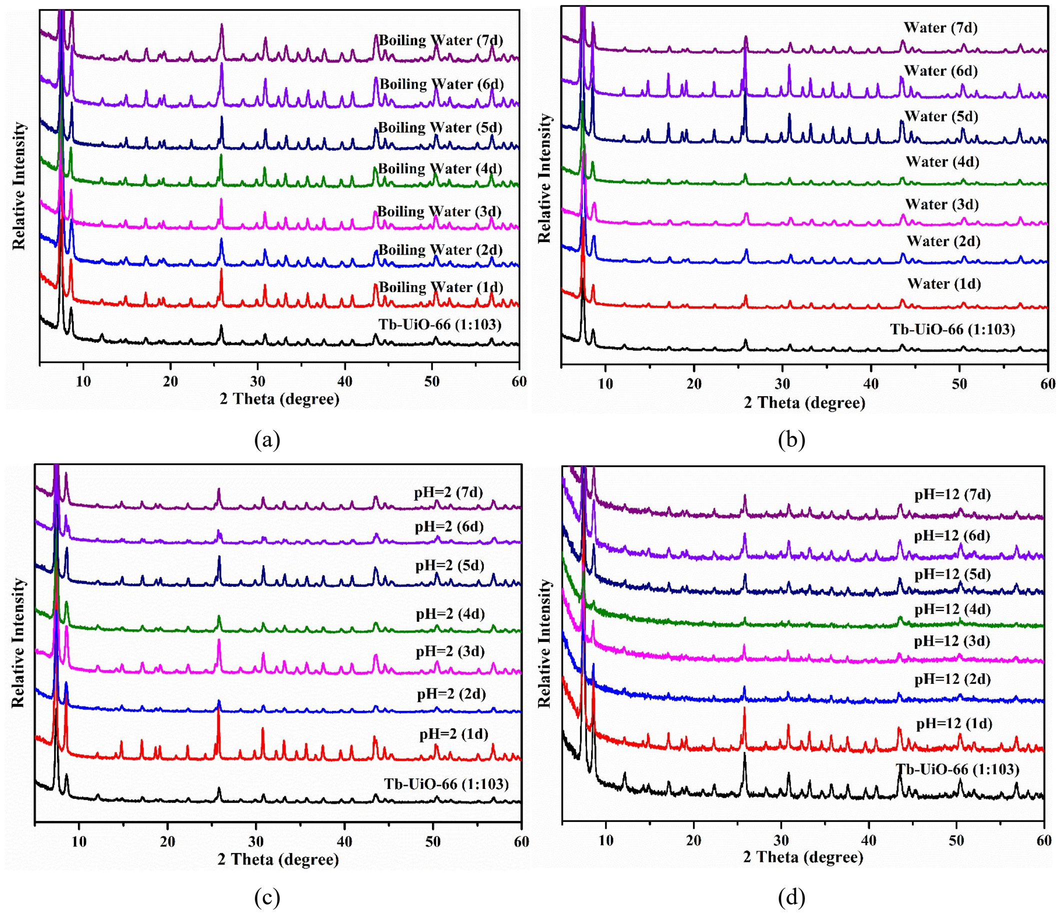

Fig. S1 PXRD patterns of Tb-UiO-66 (1:103) (a) in boiling water; (a) in ambient water; (c) in pH=2 aqueous solution at room temperature; (d) in pH=12 aqueous solution at room temperature.

Table S2. The diffraction peaks of UiO-66 and Tb-UiO-66.

Samples	2 Theta (°)		
	110	002	244
Tb-UiO-66 (1:1.5)	7.39	8.50	25.7
Tb-UiO-66 (1:17)	7.43	8.52	25.7
Tb-UiO-66 (1:65)	7.45	8.54	25.8
Tb-UiO-66 (1:103)	7.45	8.58	25.8
UiO-66	7.48	8.60	25.8

5. Thermogravimetric analysis

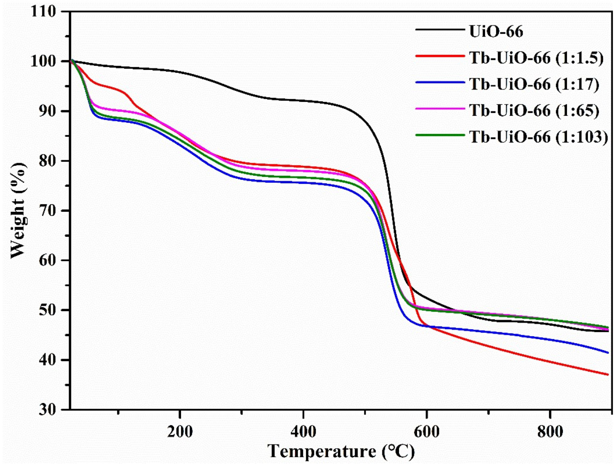

Fig. S2 Thermogravimetric analysis of UiO-66 before and after modification.

6. SEM-EDS and XPS Characterization of Tb-UiO-66

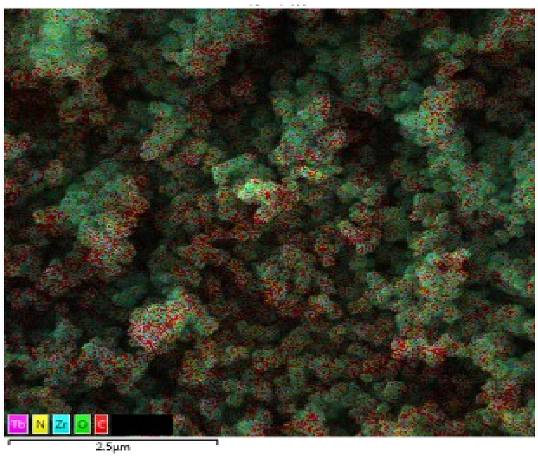

Fig. S3 SEM images of Tb-UiO-66(1:103).

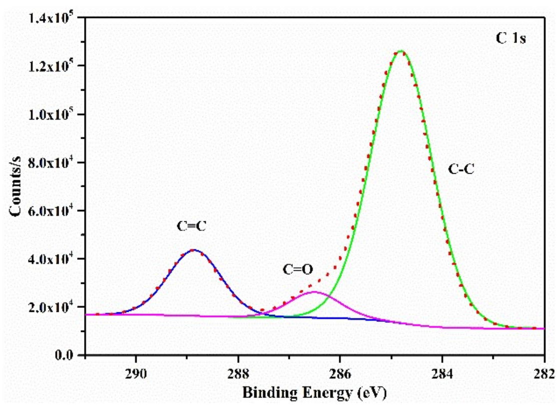

Fig. S4 XPS spectra for C 1S in Tb-UiO-66 (1:17).

Table. S3 Comparison of binding energy of Zr 3d before and after modification of UiO-66.

Samples	Zr 3d5/2	Zr 3d3/2
UiO-66	185.20 eV	182.80 eV
Tb-UiO-66 (1:103)	184.95 eV	182.60 eV
Tb-UiO-66 (1:17)	184.90 eV	182.50 eV

7. Photoluminescence properties of Tb-UiO-66

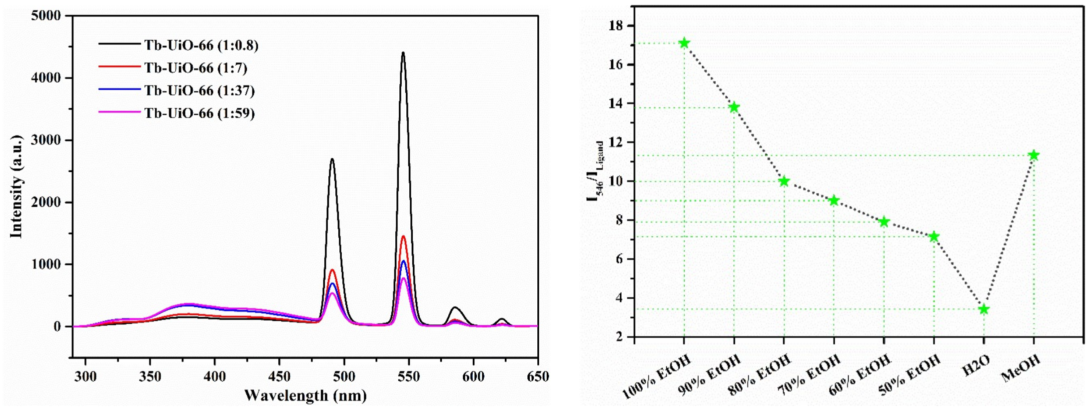

(a) (b)

Fig. S5 Tb-UiO-66 (1:103) suspended in different hydroxyl solutions (a) Emission spectra (Ex=269 nm); (b) Trend graph of relative fluorescence intensity.

8. Fluorescence sensing of styrene and EB

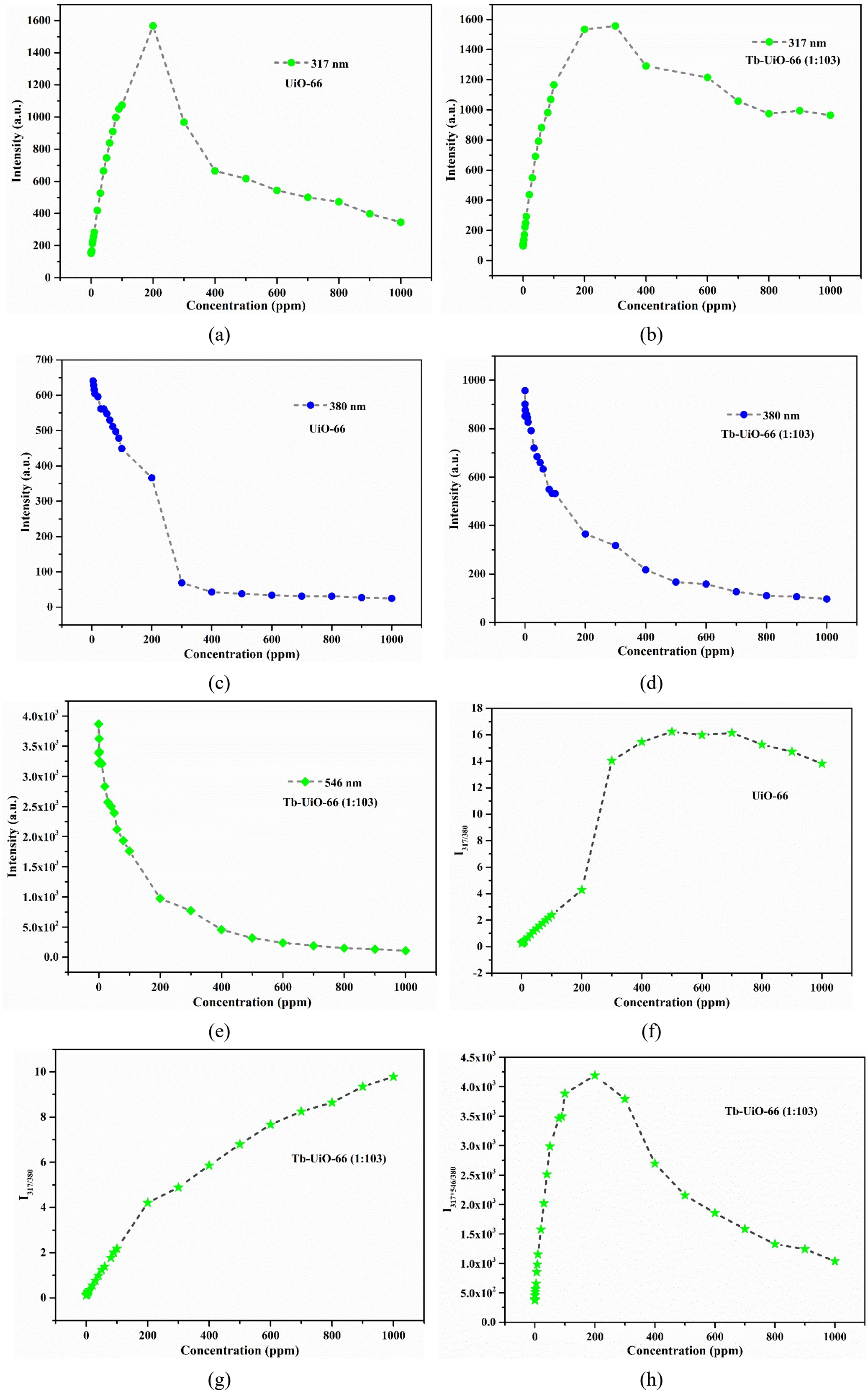

Fig. S6 (a~e) Trend diagram between styrene concentration and fluorescence intensity of UiO-66 and Tb-UiO-66 (1:103) at different emission wavelength; (f~h) Trend diagram between styrene concentration and relative fluorescence intensity of UiO-66 and Tb-UiO-66 (1:103).

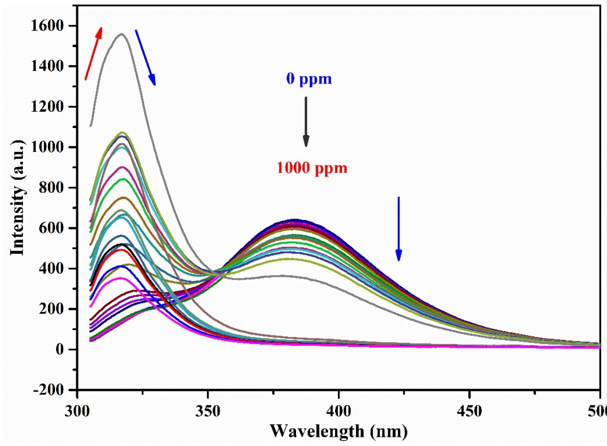

(a)

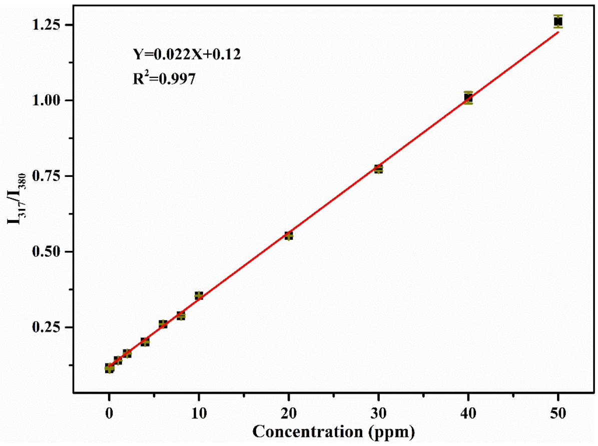

(b)

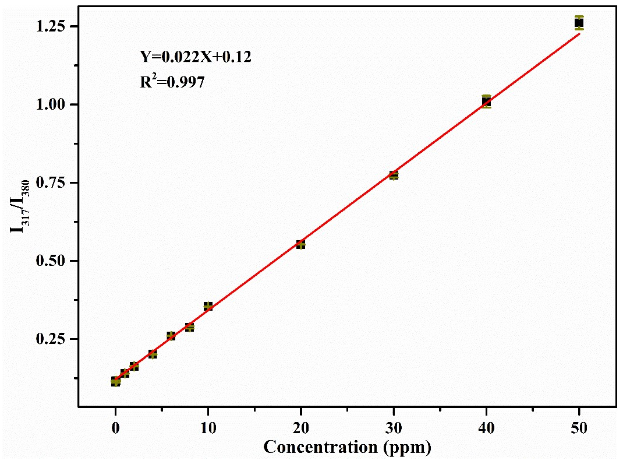

(c)

Fig. S7 Titration results of styrene (a) fluorescence spectrum of UiO-66 (λ_{ex}= 285 nm); The linear relationship of I_{317}/I_{380} with styrene concentration for UiO-66 (b) and Tb-UiO-66 (1:103) (c).

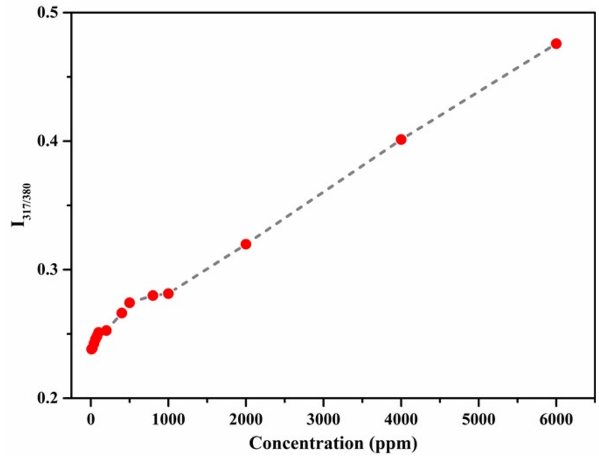

(a)

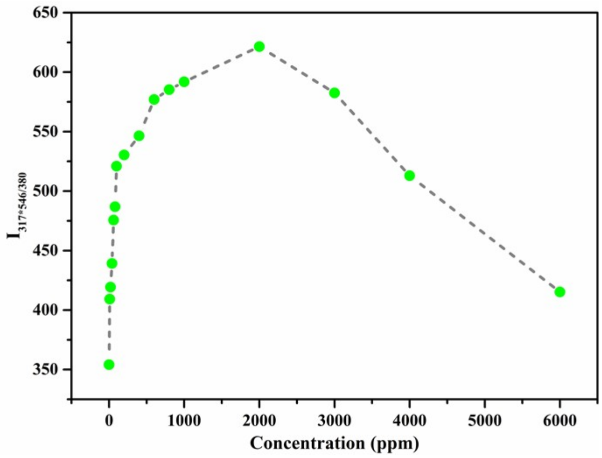

(b)

Fig. S8 The trend diagram between EB concentration and relative fluorescence intensity of (a) UiO-66 and (b) Tb-UiO-66 (1:103).

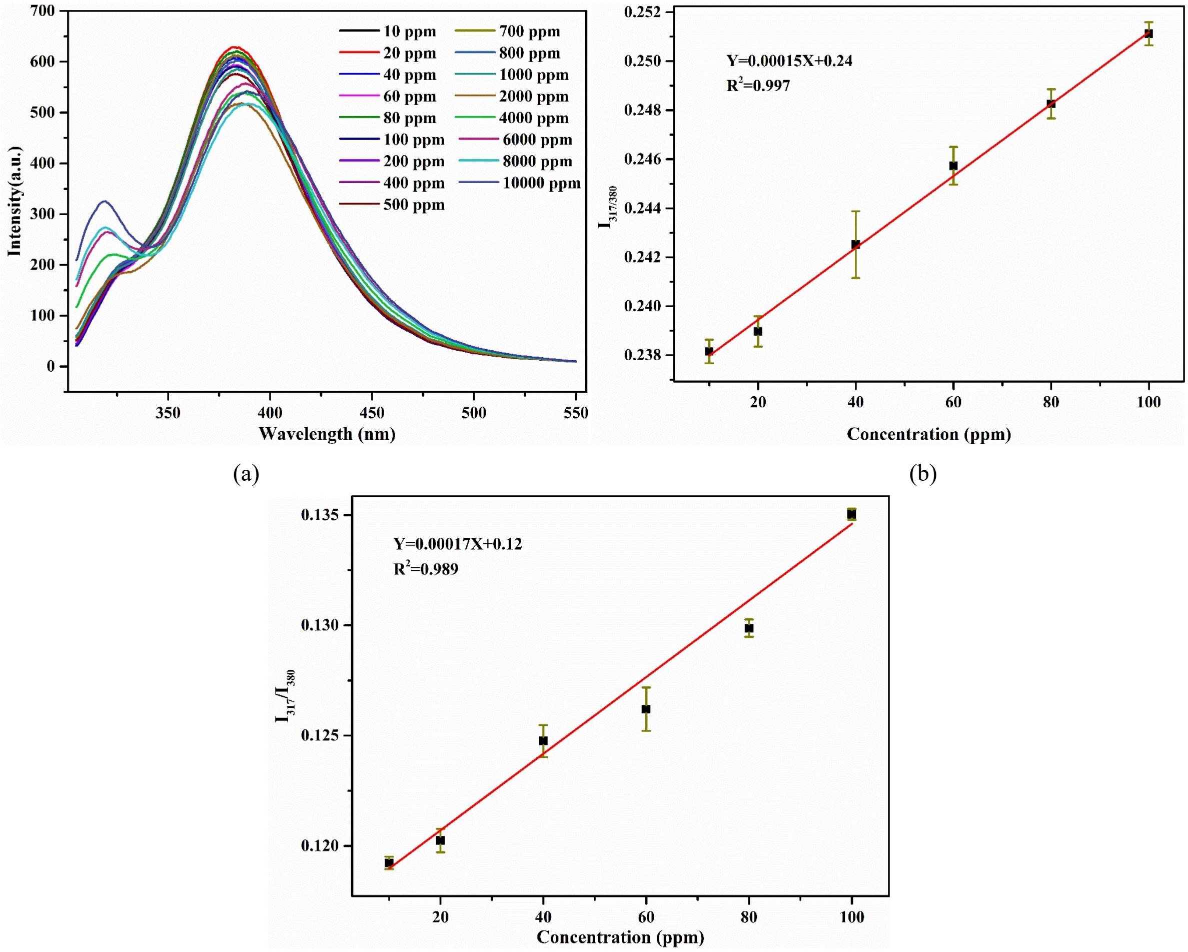

Fig. S9 Titration results of EB (a) fluorescence spectrum of UiO-66; The linear relationship of I_{317}/I_{380} with EB concentration for UiO-66 (b) and Tb-UiO-66 (1:103) (c).

Table S4. LMOFs used for the detection of styrene and EB.

No.	materials	medium used	sensor technique	LOD	VOC	Ref.
1	Tb-MOFs	methanol	Fluorescence	0.0017 %	styrene	[1]
2	UiO-66-TBPE	vapor	Fluorescence	0.706 ppm	styrene	[2]
3	ZIF-8/TiO_2	vapor	charge coupled device	57 ppm	styrene	[3]
4	PhTES-TEOS films	vapor	FTIR absorption spectra	＜100 ppm	styrene	[4]
5	NH_2-MIL-88B	vapor	photonic crystal sensor	88 ppm	ethylbenzene	[5]

9. Sensing mechanisms

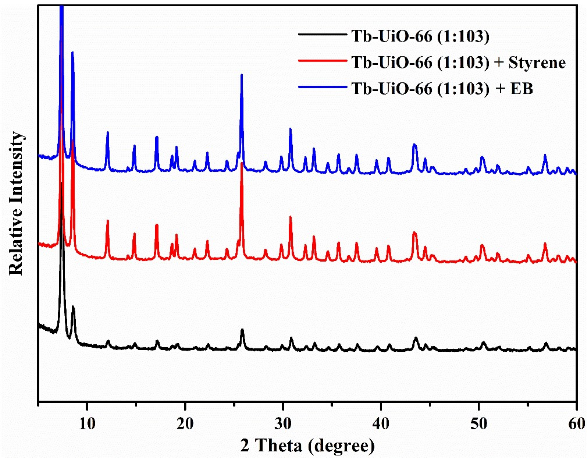

Fig. S10 PXRD patterns before and after adsorption of styrene and EB by Tb-UiO-66 (1:103).

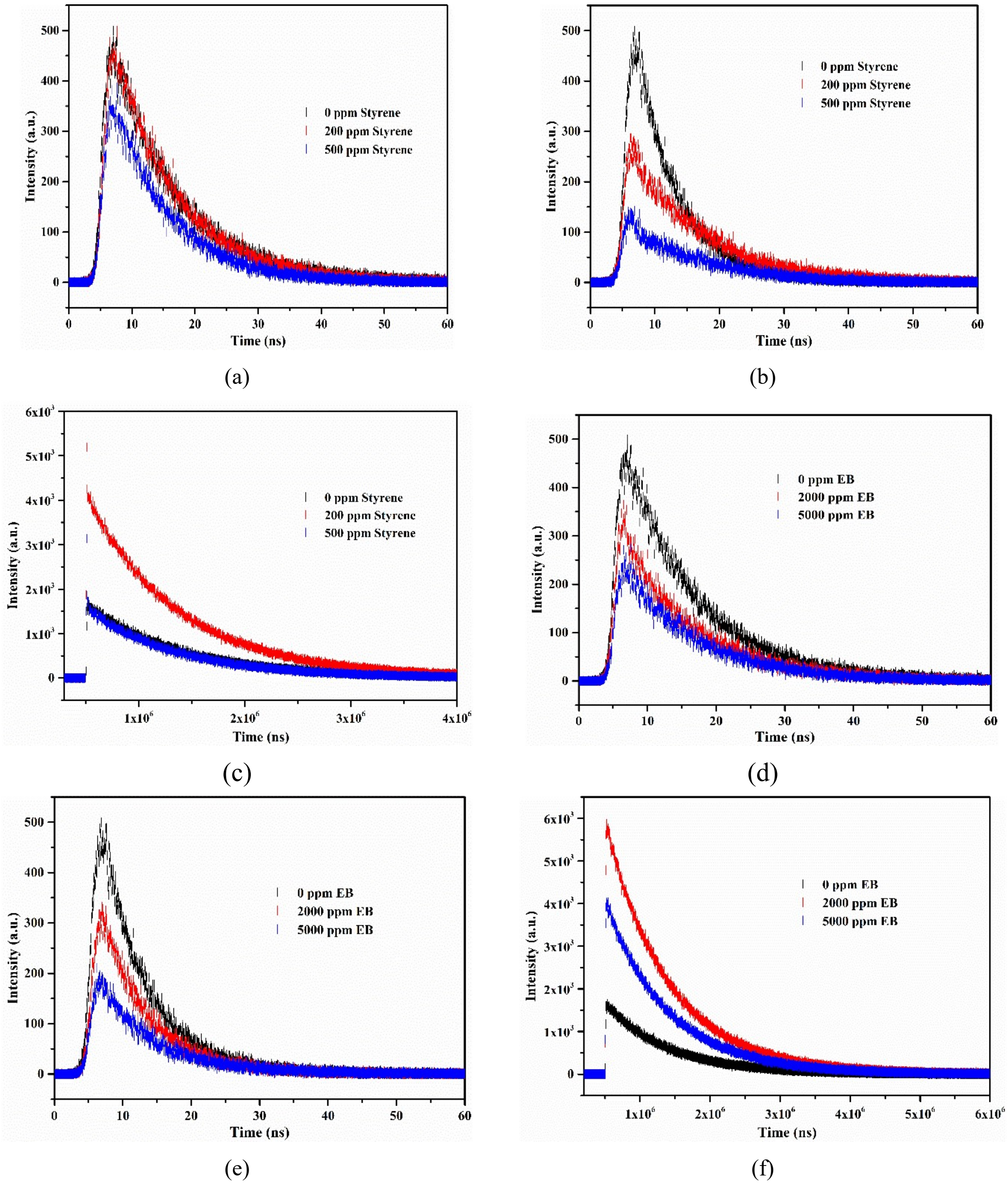

Fig. S11 Fluorescence lifetime of different styrene concentrations at different excitation wavelengths (a) 317 nm; (b) 380 nm; (c) 546 nm. And fluorescence lifetime of different EB concentrations at different excitation wavelengths (d) 317 nm; (e) 380 nm; (f) 546 nm.

Table. S5 Fluorescence lifetime parameters of different styrene concentrations at different excitation wavelengths.

Em (nm)	Concentration (ppm)	Fluorescence lifetime (τ/ns)	Energy transfer efficiency (E)	Pre-exponential factor (B_i/%)	χ^2
	0	10.2174		461.332	0.835
317	200	9.65890	5.47 %	457.775	0.834
	500	8.66000	15.2 %	347.628	0.693
	0	6.64440		478.035	0.677
380	200	10.6302	-60.0 %	269.277	0.846
	500	10.3353	-55.5 %	110.241	0.706
	0	915163		1598.94	0.975
546	200	900328	1.62 %	4002.47	1.31
	500	877557	4.11 %	1546.34	1.08

Table. S6 Fluorescence lifetime parameters of different ethylbenzene concentrations at different excitation wavelengths.

Em (nm)	Concentration (ppm)	Fluorescence lifetime (τ/ns)	Energy transfer efficiency (E)	Pre-exponential factor (B_i/%)	χ^2
	0	10.2174		461.332	0.835
317	2×10^3	10.2563	-0.381 %	299.716	0.822
	5×10^3	10.3136	-0.942 %	213.034	0.719
	0	6.64440		478.035	0.677
380	2×10^3	6.94560	-4.53 %	311.398	0.624
	5×10^3	8.06270	-21.3 %	188.467	0.736
	0	915163		1598.94	0.975
546	2×10^3	923918	-0.957 %	5651.99	1.384
	5×10^3	919322	-0.454 %	3802.81	1.199

References

1 L. Feng, C. Dong, M. Li, L. Li, X. Jiang, R. Gao, R. Wang, L. Zhang, Z. Ning, D. Gao and J. Bi, *J. Hazard. Mater.*, 2020, **388**, 121816.

2 F. Yang, J. Ma, Q. Zhu, Z. Ma and J. Wang, *ACS Appl. Mater. Interfaces*, 2022, **14**, 22510-22520.

3 O. Dalstein, D. R. Ceratti, C. Boissière, D. Grosso, A. Cattoni and M. Faustini, *Adv. Funct. Mater.*, 2016, **26**, 81-90.

4 F. Radica, S. Mura, D. Carboni, L. Malfatti, S. Garroni, S. Enzo, G. Della Ventura, G. Tranfo, A. Marcelli and P. Innocenzi, *Microporous Mesoporous Mater.*, 2020, **294**, 109877.

5 D. Kou, W. Ma, S. Zhang, R. Li and Y. Zhang, *ACS Appl. Mater. Interfaces*, 2020, **12**, 11955-11964.